Journal of Agrometeorology

ISSN : 0972-1665 (print), 2583-2980 (online)
Vol. No. 27 (1) : 49-56 (March - 2025)
https://doi.org/10.54386/jam.v27i1.2759
https://journal.agrimetassociation.org/index.php/jam

Research Paper

Assessment of air pollution resulting from the South Baghdad power plant using the Gaussian model

RUQAYA A. Al-NASER[1,*] and MONIM H. Al-JIBOORI[2]

[1]*Space Research and Technology Center, Scientific Research Commission, Baghdad, Iraq.*
[2]*Department of Atmospheric Sciences, College of Science, Mustansiriyah University, Baghdad, Iraq*
[*]*Corresponding author email:ruqaya.abdulnaser@uomustansiriyah.edu.iq*

ABSTRACT

The city of Baghdad is currently facing a significant air pollution crisis due to increased industrial activity. Therefore, the assessment of concentrations of air pollutants specifically carbon dioxide (CO_2), sulfur dioxide (SO_2), nitrogen dioxide (NO_2), nitrous oxide (N_2O), and methane (CH_4) at Al-Mustansiriya University, located approximately 10 km from the north of the South Baghdad Thermal Power Plant (SBTPP), has been made and the emission rates of these pollutants are estimated. The atmospheric stability was determined using a three-dimensional ultrasonic anemometer and stability classes were determined using the Monin-Obukhov method and applied Lagrange scale to calculate vertical and horizontal dispersion coefficients. We applied the Gaussian model to the dataset in July ٢٠٢٤, a month characterized by peak power generation and increased fuel combustion. The results showed that the vertical dispersion coefficient played an important role more than the transverse dispersion coefficient in measuring the dispersion of pollutants causing instability in the atmosphere. A significant peak around the tenth day of the month was observed, suggesting a change in winds, temperature, or weather patterns that influenced the dispersion and accumulation of these gases. The concentrations of the gases were found to vary with distance. The analysis indicated that the pollutants from the plant primarily dispersed in a north-westerly direction due to prevalent wind direction and their impact on areas near the Al-Mustansiriya University.

Keywords: Primary pollutant concentration, Atmospheric stability, Lagrangian dispersion coefficients, Effective height, and South Baghdad Thermal Power Plant.

Air pollution represents a significant environmental and public health challenge globally, with power plants being major sources of air pollutants. The city of Baghdad is currently facing a significant air pollution crisis due to increased industrial activity particularly the South Baghdad Thermal Power Plant (SBTPP). The SBTPP has garnered particular scrutiny due to its substantial emissions, which encompass a range of harmful pollutants like sulfur dioxide (SO2), carbon dioxide (CO_2), nitrous oxide (N_2O), nitrogen dioxide (NO_2), and methane (CH_4). These emissions not only degrade local air quality but also contribute to the formation of ground-level ozone and smog, which adversely affect respiratory and cardiovascular health. The geographical reach of these pollutants extends far beyond their release points, impacting air quality in distant regions. This necessitates a comprehensive understanding of the emission rates and their subsequent dispersion, facilitated by advanced modeling approaches (Younes *et al.,* 2019). Recent research highlights Iraq's vulnerability to climate change, exacerbated by factors such as rising temperatures, decreased rainfall, and the increased frequency of extreme weather events. Widespread emissions from various sources including industrial facilities, automotive exhaust, power generation, and oil refining often surpass international air quality standards (Ali *et al.,* 2024; Abdel-Razzaq *et al.,* 2023). Therefore, addressing the intersection of power generation and environmental sustainability remains a pressing concern for researchers and policymakers alike, aimed at mitigating the environmental and health repercussions linked to air pollution (Santos *et al.,* 2018; Larki *et al.,* 2023; Nasser *et al.,* 2024). The Gaussian plume model has been widely used due to its simplicity and effectiveness in estimating the concentrations of pollutants based on the distance from the source, the emission

Article info - DOI: *https://doi.org/10.54386/jam.v27i1.2759*
Received: 30 September 2024; Accepted: 22 January 2025; Published online : 1 March 2025

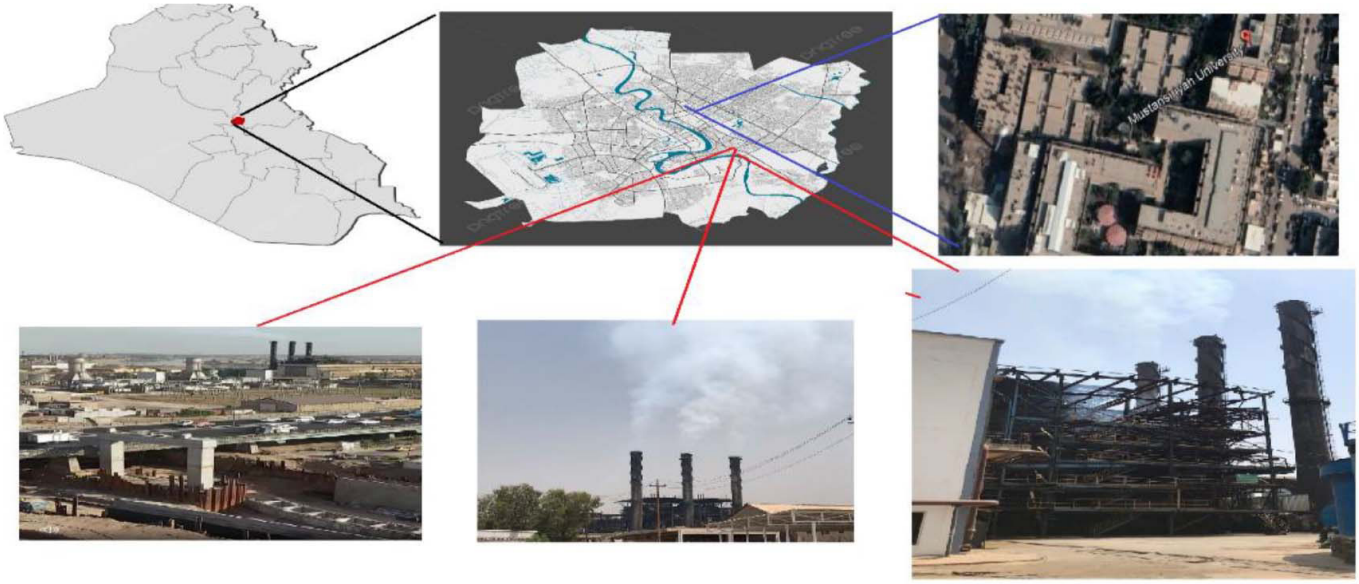

Fig. 1: Maps of Iraq and Baghdad City, and photographs for the study site (Mustansiriyah University, and South Baghdad Thermal Power Plant at the bottom).

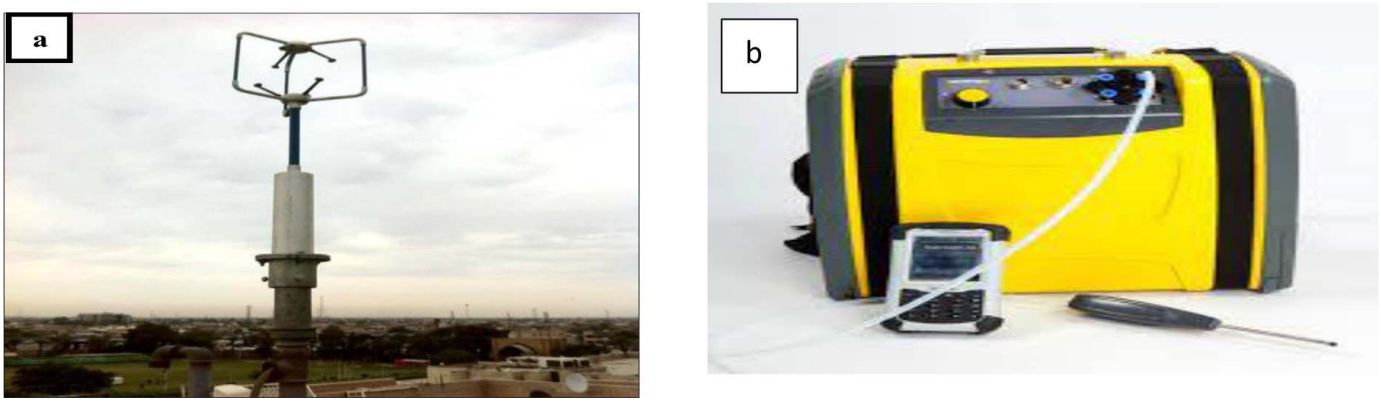

Fig. 2: (a) 3D Ultrasonic anemometer and (b) Gasmet DX4040 FTIR Gas Analyzer.

rates, and the meteorological variables such as wind speed, wind direction, and temperature. The usefulness of the Gaussian plume model in environmental assessment, particularly in understanding the distribution of pollutants and mitigating air quality problems associated with industry; al emissions has been demonstrated by several researchers (Ajayi *et al.,* 2021; Khan and Hassan, 2020; Issakhov *et al.,* 2020).

This is the first study for this power plant in terms of air pollution assessment and it aimed to evaluate the air dispersion from the South Baghdad Power Plant using the Gaussian model.

MATERIALS AND METHODS

Study location

Baghdad, located at 33.14° latitude and 44.20° longitude, is divided by the Tigris River into Karkh (west) and Rusafa (east). It features modern neighborhoods with low-rise buildings and green spaces. The study site at Mustansiriyah University has a surface roughness length of about 1-2 meters. The South Baghdad Thermal Plant, primarily fueled by fossil resources, emits pollutants including sulfur dioxide (SO_2), nitrogen dioxide (NO_2), carbon dioxide (CO_2), and methane (CH_4). Its positioning on flat terrain, near the Tigris River and populated areas, influences local air quality and pollutant dispersion. The region's semi-arid climate, with hot summers and mild winters, impacts atmospheric conditions, making it essential to understand pollutant dispersion for assessing environmental and public health effects.

Data source

We used the fast-response ultrasonic anemometer type (Wind master pro 021 - MG079141189 PK), which is located at a height of 23 meters in the Atmospheric Science Building at Mustansiriyah University, with its base at 19 meters above ground level (Fig. 2a). This instrument measures wind speed in three components: longitudinal speed (u), transverse speed (v), and vertical speed (w), with data recorded every second. The instrument collects significant data rapidly, sampling at 1 Hz and storing observations on a CD-ROM. Data collection was in July 2024. For a comprehensive analysis, observations were selected during sunrise, morning, sunset, and evening.

The concentration of pollutants was measured by the Casmet device (Fig. 2 b), which is a gas analyzer classified as a field detection device. It is a lightweight battery-operated system capable of measuring several gases (organic and inorganic) at low concentrations of parts per million (ppm) at the same time in real time. As a result of the large number of gases that can be detected by it, the device is suitable for several applications, including forensic analysis, occupational health, narcotic gases, and other applications. It is also used to detect gases, which are CO, SO_2, CH_4, CO_2, NO_2, N_2O, and many other gases. Based on these pollutants that were measured by the above device, the Gaussian model was used to estimate the extent of the impact of a power station that is 10 km away from Al-Mustansiriyah University in terms of air pollution by the above gases.

Dispersion Gaussian model

The Gaussian atmospheric dispersion model is a mathematical tool for predicting atmospheric dispersion. This model is based on the assumption that the plume of a pollutant can be predicted based on atmospheric conditions (meteorological conditions). That is, the model describes a continuous point starting from the source within a uniform (homogeneous) turbulent flow. To apply the simplified Gaussian equation, several factors have to be calculated. The first is to calculate the rate at which the pollutant gets emitted. The second is to determine the wind speed at the stack nozzle, the third is to calculate the atmospheric stability, and the fourth is to calculate vertical and transverse Lagrangian diffusion coefficients. (Anad, *et al.,* 2022)

Emission rate

The emission rate is a key parameter used to predict pollutant concentrations downwind of a source. It represents the amount of pollutants released into the atmosphere per unit of time. Data are available on the exit velocity of gases from each of the plant's three stacks, which are 55 meters high and 3 meters in diameter. Using the appropriate equation, we calculate the emission rates for the following pollutants: (SO_2, N_2O, NO_2, CH_4, and CO_2) (Al-Jiboori*, et al.,* 2024)

$$E_s\left(\frac{m^3}{sec}\right) = V_s * A = V_s * \frac{\pi * D^2}{4} \quad (1)$$

where Is the volumetric gas flow rate inside the chimney in $m^3.s^{-1}$, Vs is the exit velocity from the stack in $m.s^{-1}$, A is the area of the stack, and D is the stack diameter in m. Then we need to make the flue gas flow rate correction to take into account the moisture content and standard conditions using the following relationship:

$$E_{s.dry}\left(\frac{m^3}{sec}\right) = E_s * \frac{273.15}{T_{actual}} * \frac{P_{actual}}{1_{atm}}(1 - fracction\ water\ vapour) \quad (2)$$

T_{actual} and P_{actual} are the pressure and temperature inside the chimney in units of K and atmosphere, and by knowing the rate of concentration of a certain gas inside the chimney, we obtain the emission rate in units of $g.s^{-1}$, where the rate of gas concentrations inside the chimney was calculated from the rate of gas concentrations outside the chimney measured by the Gasmet device and divided by 2 because no analyzer inside the stack calculates the concentrations of gases inside the stack. This method was used based on the (Degrazia, 2024). If the gas concentrations are in ppm units, the emission rate is calculated using the following equation (Al-Jiboori, 2010):

$$Q_s = E_{s.dry} C_0 \rho_a \frac{\text{Mpollutant}}{\text{Ma}} \frac{1}{1000000} \quad (3)$$

where $M_{pollutant}$ is the molecular weight of the pollutant and is the molecular weight of air value 28.97 mol/mil and ρa is air density at standard conditions and its value is1.29 $kg.s^{-1}$, when substituting these values, the above equation becomes in units of $kg.s^{-1}$

$$Q_s = 4.5 * 10^{-8} * E_{s.dry} C_0\ (\text{ppm}) * M_{pollutant} \quad (4)$$

Calculation of wind at the height of stack

Wind speed was calculated based on the exponential engineering law for wind:

$$U(z) = U_r * \left(\frac{z}{zr}\right)^{\alpha} \quad (5)$$

where, U(z) is the wind speed at height (z) in $m.s^{-1}$, and Ur is the wind speed at a reference height (zr), in which the actual wind speed is measured. The exponent (α) is variable according to surface roughness and atmospheric stability. When the air reaches neutral conditions for non-rough surfaces, it is 1/7 and increases by 0.025 in urban areas. So, we employed the value of 0.025. This is because the station is located in an urban area with a height of 55 m (stack height) in this study.

Stability parameter

The M-O method was used to calculate the stability parameter following Mahmood, *et al.,* (2023). This method uses the temperature structure parameter (Z/L) to identify turbulent fluxes based on universal relationships related to atmospheric stability (Khadir *et al.,* 2024).

$$\zeta = \frac{Z}{L} \quad (6)$$

A definition of the M-O length (Al-Jiboori *et al*, 2020):

$$L = -\frac{u_*^3}{k\frac{g}{T}\overline{(w'T')}} \quad (7)$$

where *k* is the von Kármán constant (here taken to be 0.4); g is the acceleration of gravity, and the mean temperature, $\overline{(w'T')}$ Is the kinematic heat flux at the surface. The dimensionless stability was obtained by (Al-Samarrai and Al-Jiboori, 2022) and (Garratt, 1994). z is the height of the device above the earth's surface. In Eq. (7), the friction velocity (u*) is given by:

$$u* = \overline{|\ u'w'|}^{1/2} \quad (8)$$

Turbulent wind components and air temperature

The wind is inherently variable, with distinct values of the longitudinal component u(t) occurring at different times. The mean values of wind speed components are represented as ($\bar{u}$, $\bar{v}$,$\bar{w}$). The turbulence or gust component u′ can be calculated by subtracting

the mean wind from the instantaneous wind measurement. Thus, the wind consists of both mean and turbulent components (u, v, w). The three turbulent wind components (u′, v', w′) and temperature fluctuations (T′) are captured alongside their respective mean values ū, ῡ, and temperature . This relationship provides a comprehensive understanding of the wind dynamics and temperature variations within the atmospheric boundary layer as given (Stull, 2012) and (Xin *et al.,* 2002)

$$u* = \overline{|\, u'w' |}^{1/2} \quad (9)$$

Transverse and vertical Lagrangian dispersion coefficient (σ_y and σ

Dispersion coefficients represent the standard deviations in the vertical and transverse wind spreading of the concentration depending on the topography of the area of interest, atmospheric stability, distance, and time since dispersion began. The dispersion coefficients were calculated through the Lagrangian time scale, which is used to derive the dispersion coefficients for pollutants based on the time taken for the air sample to move from one location to another (Blackadar, 2012) and (Al-Naser and Al-Jiboori, 2024). The T_L is often defined using the autocorrelation function of the particle's velocity as:

$$u' = u - \bar{u};\ v' = v - \bar{v};\ w' = w - \bar{w};\ T' = T - \bar{T} \quad (10)$$

$$T_L = \int_0^{\infty} R_L(t')\, dt' \quad (11)$$

where and is the Lagrangian integral time scale. The vertical diffusion coefficient quantifies the rate at which particles diffuse in the vertical direction, which is crucial for understanding the dispersion of pollutants. It influences how pollutants, heat, and other tracers are distributed within the vertical profiles of the atmosphere. The transverse diffusion coefficient quantifies the rate at which particles diffuse in the transverse direction. These coefficients can be determined using various methodologies.

$$R_{Lv}(t') = \frac{\overline{v_L(t) v_L(t+t')}}{\overline{v_L^2}} \quad ; \quad R_L(t') = \frac{\overline{W_L(t) W_L(t+t')}}{\overline{W_L^2}} \quad (12)$$

where is the Lagrangian autocorrelation and W_L wind speed in the longitudinal direction of the particles. Where W_L wind speed in the direction vertical to the particles and is the Lagrangian autocorrelation and V_L. the wind speed to the transverse direction of the particles, and because the path is turbulent, the particle velocity is variable. Although we cannot accurately determine the path of an individual particle, we can use statistical methods to study the overall behavior of the column.

$$\sigma_y(t) = \sigma_v * (2 * T_{Lv} * t)^{1/2} \ ; \ \sigma_z(t) = \sigma_W * (2 * T_L * t)^{1/2} \quad (13)$$

where σw is the standard deviation for vertical velocity $\sigma_w^2 = \overline{w'^2}$ And σv is the standard deviation for transverse velocity. $\sigma_v^2 = \overline{v'^2}$. That has unity for $t'=0$ and zero for (t') → ∞.' The function adopted here that satisfies these requirements is:

$$\overline{V_L^2} = \sigma_V^2 \quad ; \quad \overline{W_L^2} = \sigma_w^2 \quad (14)$$

Effective stack height

Pollutants coming out of the stack rise as a result of buoyancy resulting from its heat upwards in the surrounding atmosphere, and the amount of momentum of the polluted cloud is affected by the speed of its exit. When the atmosphere is calm and neutral, atmospheric turbulence plays an important role in the vertical rise of the polluted cloud, and when the wind blows, it will interact with the vertical emission of pollutants. To simplify the subject, we assume that the dispersion of pollutants begins from an imaginary height above the chimney nozzle and not the nozzle itself, so there will be an effective height of the polluted cloud H that differs from the actual height of the chimney, which is usually greater, which is the sum of the actual height of the stack h_s (Turner, 2020)

$$H = h_s + \Delta h \quad (15)$$

where Δh, the column height can be calculated according to the amount of movement, buoyancy flux, and atmospheric stability S according to the relationship below (Haugen, 2015):

$$\Delta h = \frac{114\, S\, Fb1/3}{U_s}$$

where the Us is wind speed at stack height in units ($m.s^{-1}$) rising cloud floats on the surrounding air at a rate proportional to its cross-sectional area and its velocity relative to the surrounding air. The initial buoyancy flux Fb in units m4.s-3 is calculated by the following relationship**:**

$$F_b = \frac{g\, VsDs2}{4\, Ta}(T_p - T_a) \quad (16)$$

where Ds stack nozzle diameter unite (m) and Vs the velocity of pollutants exiting the source mouth, Tp is smoke cloud temperature unit K and Ta is the air temperature unit K. Since the station is a point source with a height H above the ground, the concentrations (C) in units $mg.m^{-3}$ with the away wind is calculated using the Gaussian model equation (Al-Jiboori *et al.,* 2024) :

$$C\ (x.0.0) = \frac{Q_s}{2\pi\ U\ \sigma y \sigma z}\ e^{-} \quad (17)$$

RESULTS AND DISCUSSION

Stability behavior in the atmosphere

In urban environments, turbulence data is critical for wind engineering and dispersion modeling. Unfortunately, there is no direct measure of stability at the station site because security is difficult, This study used criteria such as an observation height of 19 meters and data collection from an ultrasonic anemometer device during various times (sunrise, daytime, sunset, and night) to capture multiple runs within the boundary layer, particularly focusing on neutral and near-neutral conditions (±0.1). Raw data were processed to obtain three-dimensional velocity fluctuations (u′, v′, w′) and temperature fluctuations (T′) from Eq. (9), by subtracting mean values from instantaneous measurements. After filtering out unreliable data, a master dataset was created, reflecting fluctuations over 15 minutes. Stability was assessed using the dimensionless stability parameter Z/L using Eq. (14 and 15) with results from

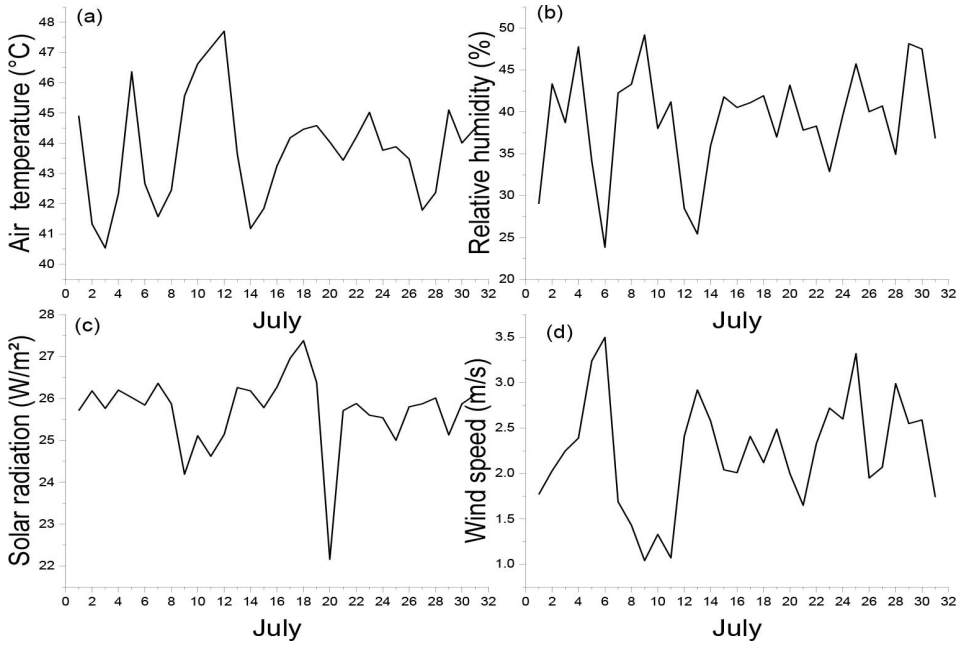

Fig. 3: (a) air temperature, (b) relative humidity, (c) solar radiation, and (d) wind speed during July 2024

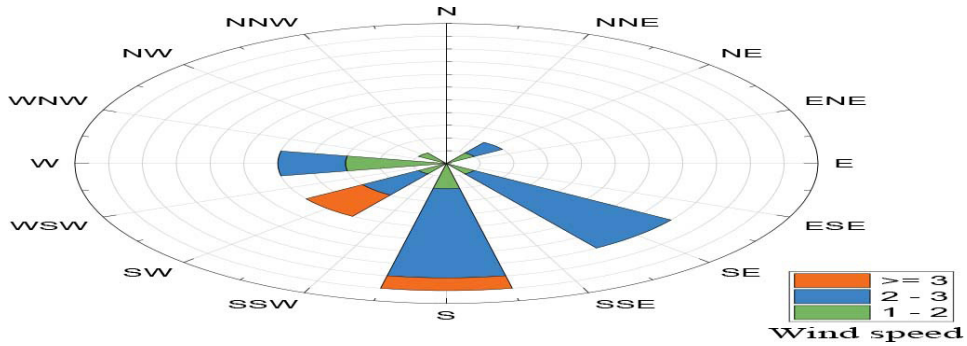

Fig. 4: A wind rose, daily wind speed and direction, July 2024.

72 runs indicating stable, neutral, and unstable conditions (Table 1). The relative frequencies of different stability ranges were as follows: Very unstable conditions (Z/L < -5) occurred 11% of the time during the day; moderate and slightly unstable regimes were 16% and 51%, respectively; neutral and moderate cases were rarer at 4%, and very stable conditions occurred 6% of the time, primarily at dawn (Table 1). This rarity of neutral conditions is attributed to continuous surface heating or cooling.

Table 1: Mean values for Z/L and standard deviation

Z/L ranges	Stability type	Z/L±SD	Frequency (%)
< (-5)	Very unstable	-4.34±1.1	11
(-1) - (-3)	Moderate unstable	-2.27±1.1	16
(-0.1)- (-1)	Slightly unstable	-0.71±0.3	51
(-0.1)- 0.1	Neutral	0.01±0.2	4
1-3	Moderat stable	2.39±0.8	4
>5	Very stable	55.76±63.6	6

Daily meteorological variables

Fig. 3 shows the time series data of air temperature, relative humidity, solar radiation and wind speed for July 2024. Fig 3(a) illustrates variations in air temperature ranging from 43 to 47 °C. The variations in relative humidity values ranged from 25% to 48%. The solar radiation varies from 22 to 27 $W.m^{-2}$, while the wind speed varies from 1.0 $m.s^{-1}$ to 3.6 $m.s^{-1}$. These graphs are an illustration of the temporal variation of each meteorological parameter for the month. The observed variations are influenced by a combination of diurnal cycles and atmospheric conditions. These are crucial for understanding the prevailing weather and climate patterns.

Wind rose analysis

During July the dominant wind direction may appear to be southeast. This is because the wind speed from the south is the strongest. Because the wind is weaker in other directions, such as north-west, the bars will be smaller (Fig. 4).

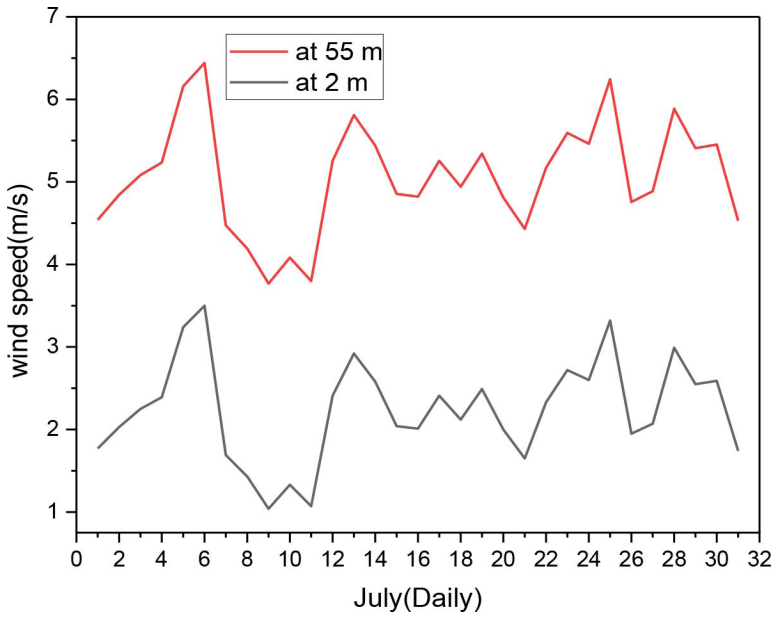

.**Fig. 5**: Wind speed is calculated at stack height according to power law

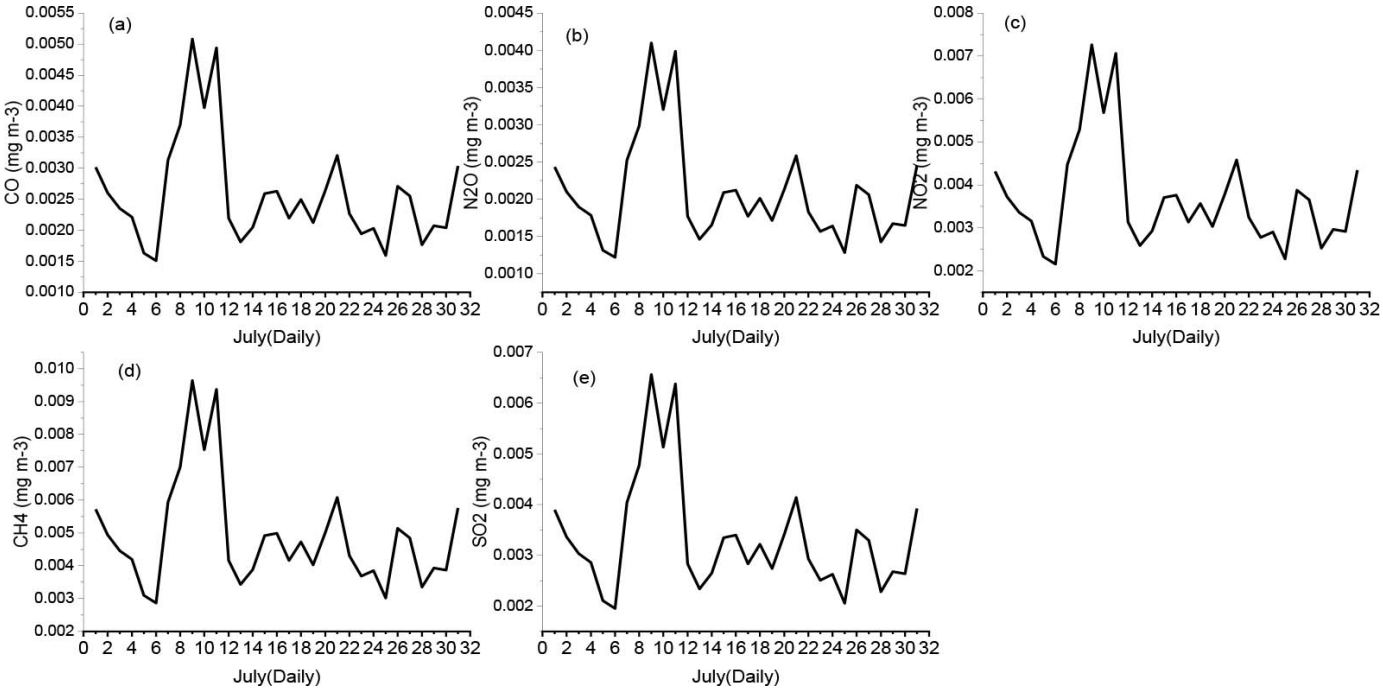

Fig. 6: Daily predicted concentration of (a)CO, (b)N_2O, (c) NO_2,(d) CH_4,(e) SO_2 with a distance of 10 km.

Estimation of gaseous CO_2, SO_2, NO,N_2O and CH_4 concentrations

The South Baghdad Thermal Power Plant (SBTPP) is located in the south of Baghdad about 10 km away from Al-Mustansiriya University, which means that roughness elements are present. Therefore, the exponential wind law was used to calculate the wind speed at a chimney height of (55 m). Fig. 5 shows the wind speed measurements at two heights (2 m), and (55 m). By the general principle that wind speed increases with height due to reduced friction with the ground, the figure shows the daily differences in wind speed throughout July with fluctuations at both heights. This figure is useful for understanding how wind speed changes with height, which is important for applications such as wind turbine siting and atmospheric modeling.

Application of simplified Gaussian model

The Gaussian model equation, specifically Eq (17), is utilized to calculate the dispersion of various gases at a distance of 10 km. During July 2024, emission rates were applied to the five pollutants in this model equation. Fig.6 (a) shows daily CO concentrations in July with significant fluctuations. The

concentrations start at around 3 mol m^{-3}, peak at 0.0055 mg m^{-3} on the 8th day, and then fluctuate between 0.0055 and 0.0015 mg m^{-3}, with a further peak on the 28th day. The peaks may be due to localized emission events (e.g., industrial activity) or to atmospheric inversions that trap CO. The variations suggest that meteorological factors such as wind and temperature have an impact on CO levels. Overall, emissions appear to be stable, but external factors cause periodic spikes. This highlights the importance of understanding emissions and atmospheric conditions to manage air quality. These values are well below the national ambient air quality standard of 960 mg m^{-3}

The predicted daily concentrations of N_2O at a distance of 10 km from a stack during July shows (Fig. 6b) that the concentration rises and peaks around the 9th and 10th days (0.0045 mg m^{-3}), then decreases, indicating improved atmospheric dispersion, and fluctuates around 0.0020 mg m^{-3} by the middle of the month. Concentrations rise again, possibly due to changes in emissions or weather, towards the end of the month. These fluctuations suggest that both emissions and meteorological factors such as wind speed and direction have a strong influence on N_2O dispersion. These values are well below the national ambient air quality standard of 647.9 mg m^{-3}

Fig. 6 (c) shows the predicted daily nitrogen dioxide (NO_2) concentrations during July, starting at around 0.005 mg m^{-3}, decreasing slightly, and then increasing sharply, peaking around 10 July at 0.007 mg m^{-3}. After this peak, there is a noticeable fluctuation in the values between 0.002 mg m^{-3} and 0.003 mg m^{-3}. Concentrations stabilize towards the end of the month, with a slight increase around the 30th day. The sharp increase in NO_2 concentration during the first third of the month could be due to increased emissions from industrial or traffic sources, weather conditions favoring the dispersion of pollutants, or changes in wind patterns. A return to more stable environmental or emission conditions is indicated by the stabilization towards the end of the month. These values are well below the national ambient air quality standard of 4800 mg m^{-3}.

The daily predicted concentrations of methane (CH_4) over July at a distance of 10 km starts at about 0.004 mg m^{-3}, decreases slightly in the first few days, and peaks at about 0.009 mg m^{-3} on day 10 (Fig. 6 d). The concentration then fluctuates with small peaks and troughs between 0.004 and 0.007 mg m^{-3}. Increased methane emissions from sources such as agriculture, landfills, or industrial activities could account for the initial sharp rise in CH_4 concentrations. The gradual increase at the end could indicate either sustained emissions or environmental conditions conducive to methane accumulation. These variations reflect the complex interplay between emission sources and atmospheric dynamics over time. These values are well below the national ambient air quality standard of 1433.6 mg m^{-3}.

The daily predicted SO_2 concentrations at 10 km shows that the concentrations start at around 0.003 mg m^{-3}, and then reach a sharp peak at around 0.0065 mg m^{-3} on the 10th day. After that, the concentrations fluctuate between 0.002 and 0.005 mg m^{-3}. There is a slight increase towards the end of the month. The peak around the 10th day suggests a temporary increase in SO_2 emissions. This could be due to industrial activities or power plant operations. The fluctuations observed thereafter are probably due to atmospheric conditions such as wind, temperature changes, or air pressure, which have an impact on the dispersion of pollutants. The slight increase towards the end of the month could be due to recurring emissions or atmospheric phenomena such as temperature inversions, which can trap the pollutants close to the ground and increase the concentrations. These values are well below the national ambient air quality standard of 150 mg m^{-3}.

CONCLUSION

The findings indicate that ground-level emissions at 10 km distance are below the National Ambient Air Quality Standards. The university is not significantly affected by the plant due to its geographical location and the prevailing meteorological conditions, which minimize pollutant transport to the campus. The prevailing winds and the distance result in significant dispersion and dilution of emissions, reducing their potential impact on air quality and health. However, the aging or poorly maintained equipment at the station contributes to incomplete combustion, which may lead to variations in emission rates due to differences in the quality of the natural gas used.

ACKNOWLEDGMENT

The authors would like to thank Al-Mustansiriya University for providing all the required facilities. They also thank the South Baghdad Thermal Power Plant for providing access to the pollutant data monitored by their devices. They also thank the Ministry of Higher Education and Scientific Research, Scientific Research Authority, and Space Research and Technology Center for providing access to the gas met device for field detection of gas emissions.

Conflict of Interest: The authors declare that there is no conflict of interest regarding this article.

Data availability: The data on daily changes in weather systems, wind speed and direction, solar radiation, temperature, and relative humidity for July of the year 2024 were obtained from the data of the Ministry of Agriculture, Agricultural Meteorology Center, Abu Ghraib Station, Baghdad Governorate.

Authors contribution: **Ruqaya A. Al-Naser** and **Monim H. Al-Jiboori**: Contributed to the design and implementation of the research, analysis of the results, and writing of the manuscript.

Disclaimer: The contents, opinions, and views expressed in the research article published in the Journal of Agrometeorology are the views of the authors and do not necessarily reflect the views of the organizations they belong to.

***Publisher's Note*:** The periodical remains neutral about jurisdictional claims in published maps and institutional affiliations.

REFERENCES

Abdel-Razzaq, F. A.-W., Yaseen, S. K. and Dhaigham, A. A. R. (2023). Design and construction of an air pollution detection system using a laser beam and absorption spectroscopy. *Baghdad Sci. J.,* 20(3): 0825-0825

Ajayi, O., Ngene, B. and Ogbiye, S. (2021). Plume Model: A Simple Approach to Air Quality Control. Paper presented at the *IOP Conf. Ser.: Mater. Sci. Eng.,* doi:10.1088/1757-899X/1036/1/012017

Ali, S. H., Qubaa, A. R. and Al-Khayat, A. B. M. (2024). Climate Change and its Potential Impacts on the Iraqi Environment: Overview. In *IOP Conf. Ser.: Earth Environ. Sci.,* (Vol. 1300, No. 1, p. 012010). IOP Publishing. doi:10.1088/1755-1315/1300/1/012010

Al-Jiboori, M. (2010). Determining of neutral and unstable wind profiles over Baghdad City. *Iraqi J. Sci.,* 51(2): 343-350.

Al-Jiboori, M. H., Al-Shaeer, M. A. and Hassan, A. S. (2020). Statistical forecast of daily maximum air temperature in arid areas in the summertime. *J. Math. Fundam. Sci.,* 52(3): 353

Al-Jiboori, M. H., Hasson, A. F. and Muhammed, N. A. (2024). Practical air pollution (p. 168). S. Press.

Al-Naser, R. A. and Al-Jiboori, M. H. (2024). Study of the vertical dispersion coefficient of air pollution under different atmospheric stability conditions over Baghdad. *Asian J. Water Environ. Pollut.,* 21(6): 173-180.

Al-Samarrai, H. M. and Al-Jiboori, M. H. (2022). Estimation of the Daily Maximum Air Temperature for Baghdad City Using Multiple Linear Regression. *Al-Mustansiriyah J. Sci.,* 33(4): 9-14.

Anad, A. M., Hassoon, A. F. and Al-Jiboori, M. H. (2022). Assessment of air pollution around Durra refinery (Baghdad) from emission NO2 gas in April Month. *Baghdad Sci. J.,* 19(3): 0515-0515. https://doi.org/10.21123/bsj.2022.19.3.0515

Blackadar, A. K. (2012). Turbulence and diffusion in the atmosphere: lectures in Environmental Sciences: Springer.

Degrazia, G. A., Stefanello, M., Costa, F. D., Martins, L. G. N. and Acevedo, O. C. (2024). Asymptotic solution for turbulent variances: application to convergence of averages and particle dispersion, *Acad. Environ. Sci. Sustain.,* 1(1) https://doi.org/10.20935/AcadEnvSci6217

Garratt, J. R. (1994). The atmospheric boundary layer. *Earth-Sci. Rev.,* 37(1-2): 89-134.

Haugen, D. (2015). Lectures on air pollution and environmental impact analyses: Springer.

Issakhov, A., Omarova, P. and Issakhov, A. (2020). Numerical study of thermal influence to pollutant dispersion in the idealized urban street road. *Air Qual. Atmos. Health,* 13, 1045-1056.

Khadir, J. M., Hassoon, A. F. H. and Al-Knani, B. A. (2024). Influence of atmospheric stability conditions on wind energy density in Ali Al-Gharbi region of Iraq. *J. Agrometeorol.,* 26(3): 279-289. https://doi.org/10.54386/jam.v26i3.2589

Khan, S. and Hassan, Q. (2020). Review of developments in air quality modeling and air quality dispersion models. *J. Environ. Eng. Sci.,* 16(1): 1-10. https://doi.org/10.1680/jenes.20.00004

Larki, I., Zahedi, A., Asadi, M., Forootan, M. M., Farajollahi, M., Ahmadi, R. and Ahmadi, A. (2023). Mitigation approaches and techniques for combustion power plants flue gas emissions: A comprehensive review. *Sci. Total Environ,* 166108. https://doi.org/10.1016/j.scitotenv.2023.166108

Mahmood, D. A., Naif, S. S., Al-Jiboori, M. H. and Al-Rbayee, T. (2023). Study the relationships among stability parameters in the atmospheric surface layer adjacent to an oil refinery, in Baghdad. AIP Conf. Proc.

Nasser, M. S., Al-Hassany, J. S. and Al-Jiboori, M. H. (2024). Assessment of air pollution dispersion during wet season: A case study of Rumaila Combined Cycle Power Plant, Basrah, Iraq. *J. Agrometeorol.,* 26(4):411-418. https://doi.org/10.54386/jam.v26i4.2756

Santos, L. G. R., Afshari, A., Norford, L. K. and Mao, J. (2018). Evaluating approaches for district-wide energy model calibration considering the Urban Heat Island effect. *Appl. Energy*, 215:31-40. https://doi.org/10.1016/j.apenergy.2018.01.089

Stull, R. B. (2012). An introduction to boundary layer meteorology (Vol. 13): Springer Science and Business Media.

Turner, D. B. (2020). Workbook of atmospheric dispersion estimates: an introduction to dispersion modeling: CRC press.

Xin, L., Fei, H., Yifen, P., Al-Jiboori, M., Zhaoxia, H. and Zhongxiang, H. (2002). Identification of coherent structures of turbulence at the atmospheric surface layer. *Adv. Atmos. Sci.,* 19: 687-698.

Younes, M., Harale, A., and Musawi, M. (2019). Process for acid gas treatment and power generation. In: Google Patents.